Carbohydrate Polymers 111 (2014) 133–138

Contents lists available at ScienceDirect

Carbohydrate Polymers

journal homepage: www.elsevier.com/locate/carbpol

Effect of retrogradation time on preparation and characterization of proso millet starch nanoparticles

Qingjie Sun*, Min Gong, Ying Li, Liu Xiong

School of Food Science and Engineering, Qingdao Agricultural University, Qingdao, Shandong Province, 266109, China

ARTICLE INFO

Article history:
Received 26 December 2013
Received in revised form 27 March 2014
Accepted 28 March 2014
Available online 5 April 2014

Keywords:
Proso millet starch
Starch nanoparticles
Debranching
Recrystallized
Retrogradation

ABSTRACT

Starch nanoparticles were prepared from proso millet starch using a green and facile method combined with enzymolysis and recrystallization. Scanning electron microscopy (SEM), X-ray diffraction (XRD), Fourier transform infrared spectroscopy (FTIR), differential scanning calorimeter (DSC) and thermal gravimetric analysis (TGA) were used to characterize the morphology and crystal structure of the starch nanoparticles prepared with different retrogradation time (0.5, 4, 12, and 24 h). The results showed that the sizes of the starch nanoparticles were between 20 nm and 100 nm. The crystal pattern changed from A-type (native starch) to B-type (nanoparticles), and the relative crystallinity of the nanoparticles increased obviously, as compared with the native starch. The nanoparticles prepared with the 12 h retrogradation time had the highest degree of crystallinity (47.04%). Compared to conventional acid hydrolysis to make starch nanoparticles, the present approach has the advantage of being quite rapid and presenting a higher yield (about 55%).

1. Introduction

As an abundant, inexpensive, naturally renewable, and biodegradable polysaccharide, starches are widely used in many industries especially food products. In recent years small-sized starch granules or particles have been attracted attention because of their novel physical properties, for example, the capability of holding various sensitive materials such as food flavors (Tari, Annapure, Singhal, & Kulkarni, 2003). Kim and Lim (2009) reported that small starch granules can mimic lipid micelles, providing a fat-like texture. Starch nanoparticles composed of platelet crystallites (20–40 nm long and 15–30 nm wide) have also been obtained from waxy maize starch using selective acid hydrolysis (Putaux, Molina-Boisseau, Momaur, & Dufresne, 2003). Furthermore, the nano-sized starch particles have been used as potential fillers for natural rubber because of their increased reinforcing effect (Angellier, Molina-Boisseau, & Dufresne, 2005). Starch nanoparticles are usually obtained from acidic or enzymatic hydrolysis and consist mainly of small blocklets (Kim & Lim, 2008; Putaux et al., 2003). In addition to acid hydrolysis, chemical or enzymatic agents may also be used to destruct, oxidize, or derivatize the starch to make starch nanoparticles. By selective enzymatic hydrolysis, nano-scale starch particles with average diameters of 500 nm were prepared form waxy rice starch (Kim & Lim, 2008).

Pullulanase (pullulan 6-glucanohydrolase, EC 3.2.1.41), which rapidly hydrolyzes only the α-1,6-glycosidic bonds, releasing a mixture of linear shorter chains of glucose units from the parent amylopectin molecule, has been gaining importance in starch conversion processes (Shi, Chen, Yu, & Gao, 2013; Lin & Chang, 2006). Usually, enzymes used for starch hydrolysis are utilized in the water system, and the hydrolysis requires pre-swelling the starch in water and full starch gelatinization. After debranching amylopectin with pullulanase, amylopectin can be hydrolyzed into a lot of short linear glucans, which can re-associate and subsequently retrogradate. Occasionally, branched short linear glucans can easily reassemble into nano-scale starch at a low temperature; however, most reports on debranching with pullulanase studied the slowly digestible starch (SDS) content or resistant starch after hydrolysis (Milasinovic, Radosavljevic, & Dokic, 2010). Few studies have been performed in the preparation of the nano-scale starch particles with pullulanase debranching. Publications about the preparation of starch nanoparticles through enzymolysis and recrystallization have been rarely reported.

Proso millet (*Panicum miliaceum* L.), which is also called millet, hog millet, and yellow hog, has excellent nutritional properties and can become a basic resource for crop breeding programs and food diversification (Yañez, Walker, & Nelson, 1991; Young-Il Cho et al., 2010). Proso millet is desirable for human food because it is

* Corresponding author at: School of Food Science and Engineering, Qingdao Agricultural University,, 700 Changcheng Road, Chengyang District, Qingdao, 266109, China. Tel.: +86 532 88030448; fax: +86 532 88030449.
E-mail address: phdsun@163.com (Q. Sun).

http://dx.doi.org/10.1016/j.carbpol.2014.03.094
0144-8617/

easily digestible and is gluten-free. Like many other starch sources, proso millet starch is comprised of two components, amylose and amylopectin, and it has been widely utilized in the food and pharmaceutical industries (Kim, Choi, Kangm, & Kim, 2012).

In this study, proso millet starch was debranched by pullulanase to produce starch enzymatic hydrolysate with linear and low molecular weight polymer chains. The solutions were then stored at 4 °C for different retrogradation time (0.5, 4, 12, and 24 h) to recrystallize into different starch nanoparticle samples. The morphology, crystalline characteristics, and thermal characteristics of the starch particles were investigated.

2. Materials and methods

2.1. Materials

Proso millet grains (Millet Lu 1) were obtained from Qingdao Academy of Agricultural Sciences, Qingdao, China. Pullulanase (E.C.3.2.1.41, 6000 ASPU/g, 1.15 g/mL) (ASPU is defined as the amount of enzyme that liberates 1.0 mg glucose from starch in 1 min at pH 4.4 and 60 °C) was obtained from Novozymes Investment Co. Ltd. (Beijing, China). All analytical-grade chemicals were used as obtained and were not further purified.

2.2. Proso millet starch preparations

The proso millet starch was prepared using the alkaline steeping method (Ju, Hettiarachchy, & Rath, 2001; Santhanee & Dudsadee, 2013) with some modifications. Proso millet grains were steeped in 0.3% sodium hydroxide solution and kept at 4 °C for 24 h. The supernatant was discarded and the steeped millets were ground with a blender and passed through a 100 mesh screen. The slurry was centrifuged at 3000 rpm for 15 min. Then, the supernatant was decanted and the precipitate was re-slurried with water and then centrifuged. The step of washing was repeated three times. Next, the starch cake was re-suspended in water, neutralized with 1 N hydrochloric acid to pH 7.0. The supernatant was decanted and the neutralized starch was removed and dried in an oven at 40 °C for 48 h. The amylose content of the starch was about 3%.

2.3. Enzymatic debranching and recrystallization

The proso millet starch (10 g) was dispersed in 100 mL of disodium hydrogen phosphate and a citric acid buffer solution (pH 5.0) to make starch concentration of 10% (w/v), which was then cooked in boiling water with vigorous stirring for 30 min to make sure that the starch fully gelatinized (An et al., 2011). The temperature of the cooked starch solution was adjusted to 56 °C and pullulanase (30 ASPU/g of dry starch) was added (Miao, Jiang, & Zhang, 2009). After 8 h enzymatic hydrolysis period to make sure that the starch chains were fully debranched, the reaction was stopped by heating at 100 °C for 30 min and then centrifuged at 3000 rpm for 15 min to remove the precipitation. The pellucid solutions were cooled to room temperature and then stored at 4 °C for different retrogradation time (0.5, 4, 12, and 24 h) to form different millet starch nanoparticle samples. The starch suspensions were centrifuged and washed several times with distilled water until neutrality and then freeze dried. The branched short linear glucans could form nano-scale starch particles during the retrogradation process. When freeze drying, water in starch nanoparticles slurry was removed directly by the ice sublimation, keeping the intact nano-scale particles. Then we obtained four starch nanoparticle samples made with different retrogradation time (0.5, 4, 12, and 24 h), respectively. The yield was calculated by dividing the weight of the freeze-dried precipitate by the initial dry weight of the millet starch.

2.4. Scanning electron microscopy (SEM)

The particle microstructure of proso millet native starch (NS) and nano-scale starch particle samples was observed with a scanning electron microscope (SEM) using the method described by Kim et al. (2008). All starch nanoparticle suspensions were deposited on a carbon-coated microscopy grid and freeze dried. The native starch was attached to an SEM stub using double-backed cellophane tape. All the samples were placed on double-sided cellophane tape and coated with a thin film of gold under a vacuum. Samples were observed under a Jeol scanning electron microscope (JSM 840, Jeol, Japan).

2.5. X-ray diffraction pattern

The crystal structure of the native and nano-scale starch samples was studied with an X-ray diffractometer (Bruker AXS Model D8 Discover) using the conditions described by Watcharatewinkula et al. (2009). Both native starch and starch nanoparticle samples were equilibrated in a saturated relative humidity chamber for 24 h at room temperature. The X-ray diffraction was performed on an X-ray diffractometer with copper Ka radiation. Signals of the reflection angle of 2θ, from 4° to 40°, were recorded.

2.6. Fourier Transform Infrared Spectroscopy (FTIR)

The infrared spectra of native and nano-scale starch samples were recorded on an FTIR spectrophotometer (NEXUS-870, Thermo Nicolet Corporation) as described by Kunal, Banthia, and Majumdar (2008). All the samples were mixed with KBr and pressed into pellets. The pellets were then subjected to attenuated total reflectance (ATR) spectroscopy in the range of 4000–400 cm^{-1}. Intensity measurements were performed on the spectra by recording the height of the absorbance bands from the baseline.

2.7. Differential scanning calorimeter (DSC)

The thermal properties of proso millet native starch (NS) and nano-scale starch particle samples produced via the enzymolysis and recrystallization described above were investigated using a differential scanning calorimeter (DSC 1, Mettler-Toledo, Schwerzenbach, Switzerland) as described by Chanvrier et al. (2007) with minor modifications. Indium was used as the calibration standard. The sample (10 mg) mixed with distilled water (20 mg) was placed in a stainless steel pan, the container was hermetically sealed, and then the sample was kept at 4 °C for 24 h. Samples were heated at 10 °C/min from 25 °C to 125 °C to watch for the presence of any peak in residual enthalpy gelatinization. The endothermic enthalpy (ΔH), onset temperature (T_o), peak temperature (T_p), and conclusion temperature (T_c) were determined.

2.8. Thermogravimetric analysis

The thermogravimetric (TG) and differential thermogravimetric (DTG) curves were obtained using a synchronous thermal analysis (STA449C/4/G, Netzsch, Germany) as described by Moreira, Pedro, Glenn, Marconcini, & Mattoso (2013) with minor modifications. Approximately 4 mg of each sample was loaded into a platinum pan and heated from 25 °C to 550 °C at a heating rate of 10 °C/min. All the measurements were performed under a dynamic atmosphere of synthetic air (80% N_2 and 20% O_2) with a gas flow of 20 ml/min in order to prevent any thermoxidative degradation. Inorganic

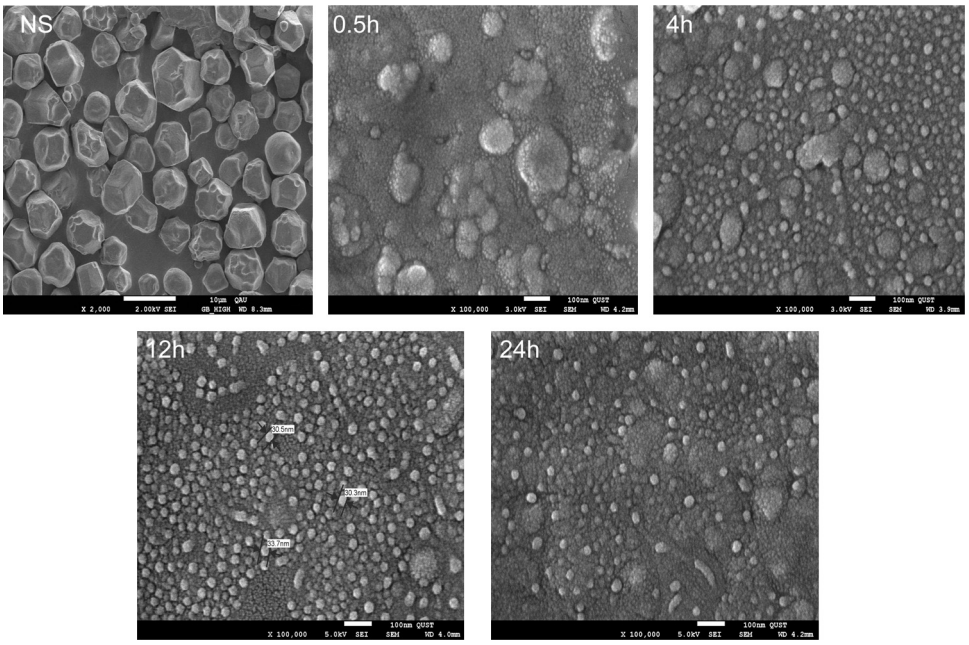

Fig. 1. SEM images of proso millet native starch (NS) and nano-scale starch particles prepared with different retrogradation time: 0.5, 4, 12, and 24 h.

content was determined by the residue left at 550 °C. Two replicates were analyzed for each sample.

2.9. Statistical analysis

All experiments were conducted at least in triplicate, with mean values and standard errors determined for these experiments. All the test data were analyzed using the analysis of variance (ANOVA) and the Origin Pro 8.0 statistics programs and then expressed as mean values ± standard deviations. Differences were considered significant at 95% ($p < 0.05$).

3. Results and discussion

3.1. Yields and morphology of nano-scale proso millet starch particles

The yield of the starch nanoparticle samples with 0.5, 4, 12, and 24 h retrogradation time at 4 °C was 15.29, 39.74, 53.94, and 54.66%, respectively. The retrogradation time had great effects on the yield of the starch nanoparticle, and the sample recrystallized for 0.5 h had the least yield among all samples. With the retrogradation time prolonged, more and more debranched short linear glucans reassembled into starch nanoparticles. The yields of recrystallized starch nanoparticles increased slightly after 12 h storage probably because of full retrogradation of debranched short amylose.

The morphology and size of proso millet native starch and nano-scale starch particles prepared with different retrogradation time (0.5, 4, 12, and 24 h) are shown in Fig. 1. The SEM of proso millet native starch granules exhibited a mixture of shapes such as oval, irregular, and polygonal, with a granule size between 3 and 9 μm. The recrystallized samples were well dispersed without aggregation, the shapes of the four samples were irregular, and the diameter size of the nano-scale starch particles prepared with different retrogradation time were different around 30–100 nm. The sample recrystallized at 4 °C for 0.5 h had lots of large starch particles that were about 100 nm in size and only a few small particles below 50 nm. With the retrogradation time prolonged (4, 12, and 24 h), smaller nano-scale starch particles about 30 nm or so in size were observed in the SEM pictures. The starch nanoparticles of the sample with a 12 h retrogradation time had a size uniformity of 30 nm. With the retrogradation time prolonged to 24 h, we observed that larger particles arose in the image. This may be attributed to the reassembling of the branched short linear glucans and the growth of starch crystallites with the longer storage time and at a lower temperature (4 °C).

The obtained nano-scale starch particles were probably due to the retrogradation of short amylose chains debranched from amylopectin. Zhang and Jin (2011) have also reported that amylopectin can be debranched by pullulanase and that the short amylose chains released from amylopectin can form double helices, which increase the density of the crystalline structure. It is well known that debranching enzymes (pullulanase) can rapidly cleave α-1,6-glycosidic bonds and give rise to a mixture of long and short unit chains from the parent amylopectin molecule. It was reported that waxy maize starch nanocrystals consisted of platelet-like particles approximately 15–500 nm wide were obtained after long time hydrolyzing (Liu, Wu, Chen, & Chang, 2009). Kim and Lim (2008) and An et al. (2011) have reported that the hydrolyzed starch was debranched into starch crystallites of 10–20 nm or even shorter starch slices. According to the crystal formation and growth mechanism reported by Geng, Jiang, and Zhu (2012), when synthesizing nanoparticles from solution, nucleation is very fast, and subsequent growth occurs by two primary mechanisms: coarsening (also known as Ostwald ripening) and growth involving aggregation. At low retrogradation time, the nucleation of shorter glucose units and slices was very fast and the larger nanoparticles may be attributed to fast aggregation of the short debranched starch chains. With the retrogradation time longer, lots of crystal nucleus grew into large numbers of nano-scale starch particles (30 nm), the initial aggregated larger nanoparticles were relatively decreased. Another possibility was that the starch nanoparticles were not fully crystallized and the distance between the glucose unites was larger initially, which accounted for the larger nanoparticles at low retrogradation time. According to Shi and Gao (2011), an appropriate chain length (DP 20–30) is required for crystallization and formation of double helices. The debranched short linear glucans from amylopectins by debranching enzymes could easily reassemble into nano-scale starch at low temperature or with longer storage time. Miao et al. (2009) found that the granular structure

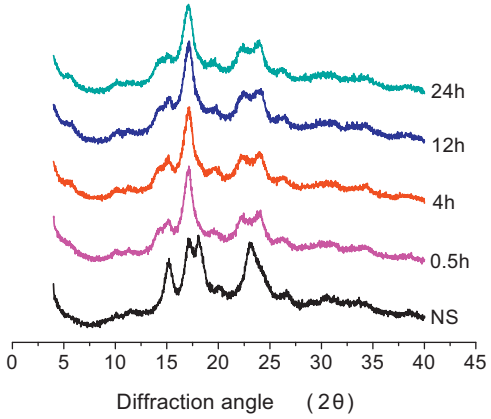

Fig. 2. X-ray patterns of proso millet native starch (NS) and nano-scale starch particles prepared with different retrogradation time: 0.5, 4, 12, and 24 h.

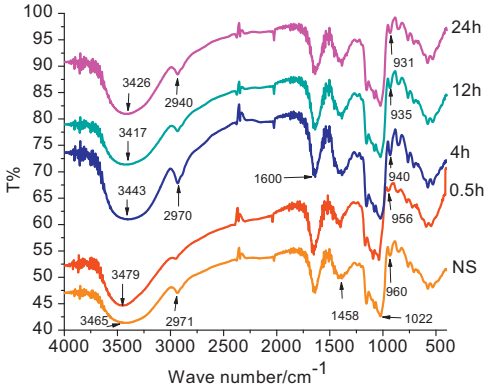

Fig. 3. FTIR spectra of proso millet native starch (NS) and nano-scale starch particles prepared with different retrogradation time: 0.5, 4, 12, and 24 h.

disappeared in cooked-debranched-stored waxy maize starch samples; further, they observed smooth, plate-like surfaces and bigger, irregularly shaped particles. Shi et al. (2013) also reported that the RS III prepared from waxy maize starch with pullulanase showed irregularly shaped fragments dried at 45 °C overnight. Zhang and Jin (2011) attributed this fact to the retrogradation of amylose chains, which resulted in a reorganization of the starch structure into a helical complex.

3.2. X-ray diffraction pattern

To study the effect of different recrystallization time on the crystalline structure of proso millet nano-scale starch particles, X-ray diffraction patterns of native starch and starch nanoparticles were observed and are shown in Fig. 2. The X-ray diffraction pattern of proso millet native starch showed the classic "A" type, which was representative of grain starches with main reflections at 2θ of 15°, 17°, 18°, and 23.5°, respectively. All recrystallized nano-scale starch particle samples displayed a typical B-type crystalline structure with main diffraction peaks at 2θ = 5.6°, 17.1°, 22.5°, and 24.3°. The characteristic diffraction peak of B-type at 2θ = 5.6° increased significantly in intensity after debranching treatment with different recrystallization time. This was a result of the reorganization of the starch chain due to retrogradation (Simsek & El, 2012). Similarly, Shi and Gao (2011) reported that native waxy rice starch was A-type, but debranched short-chain amylose recrystallized at 25 °C changed to a B-type X-ray pattern. The polymorphic structure was affected by the crystallization temperature. Reports have shown that retrogradation at 40 °C led to the formation of a B-type polymorph, whereas incubation at 95 °C produced a mixture of A- and V-type polymorphs (Shamai, Bianco-Peled, & Shimoni, 2003).

The relative crystallinity of the native proso millet starch and recrystallized starch nanoparticles at different time are summarized in Table 1. The retrogradation time had great effects on the relative crystallinity of the recrystallized starch nanoparticle samples. Compared to the crystallinity of the native starch (37.22%), all nano-scale starch particle samples had higher relative crystallinity, and the crystallinity increased with the retrogradation time that was prolonged from 0.5 h to 12 h. The recrystallized sample at 4 °C for 12 h had the highest relative crystallinity at 47.04%. The crystallinities of other samples with 0.5, 4, and 24 h retrogradation time were 42.27, 43.02, and 46.75%, respectively. After gelatinization and debranching by pullulanase, the aqueous starch solutions re-associated by forming double-helical strands along the linear sections of constituent polymer chains. These strands subsequently aggregated into ordered domains of different morphologic orientation depending on recrystallization conditions (Buleon, Veronese, & Putaux, 2007). Several reasons such as crystal size, amylopectin content and amylopectin chain length, extent of interaction between double helix, and orientation of the double helices within the crystalline domains could influence the differences in degree of crystallinity. The recrystallization of starch is a complex process involving conformational change, chain alignment, crystal packing, and phase propagation. Whereas debranching frees short linear α-(1-4) polymers that favor crystallization, the longer amylose chains associate much faster and form networks that impede propagation of substantially ordered crystallites.

3.3. Fourier Transform Infrared Spectroscopy (FTIR)

The FTIR spectrum of proso millet native starch and nano-scale starch particles prepared with different retrogradation time is shown in Fig. 3. The characteristic bands originated mainly from the vibrational modes of amylose and amylopectin. The strong absorption band in the range of 3500–3300 cm^{-1} was attributed to the O–H stretching of the starch, and the peak width indicated the extent of formation of inter- and intra-molecular hydrogen bonds. The absorption peak of recrystallized starch nanoparticle samples with different retrogradation time changed obviously from 3465 cm^{-1} (NS) to 3479 cm^{-1} (0.5 h), 3443 cm^{-1} (4 h), 3417 cm^{-1} (12 h), and 3426 cm^{-1} (24 h), respectively. The position of the peaks moved to a lower band in the recrystallized starch nanoparticle samples (except 0.5 h), indicating that there was an increase in the intermolecular force of hydroxyl groups in the starch nanoparticle samples (Lian, Liu, Guo, Li, & Wu, 2013). The irregular absorption change of 0.5 h starch nanoparticle sample may attribute to the imperfect crystallization within a short retrogradation time.

The asymmetric stretching of C–H was observed at 2971 cm^{-1}, and the absorption band at 1458 cm^{-1} was attributed to tightly bound water present in the starch (Shi, Wang, Li, & Benu, 2012). The FTIR spectrum showed a more obvious peak at about 2940 cm^{-1} to 2970 cm^{-1} (C–H stretching) after debranching and retrogradation. The absorption bands between 1000 cm^{-1} and 1200 cm^{-1} were characteristic of the C–O stretching of polysaccharide skeleton. The bands at 850 cm^{-1} and 1022 cm^{-1} were sensitive to crystallinity changes. The band intensity at 1022 cm^{-1} determined the orientation of the intermolecular H-bonding of CH and CH_2 in CH_2OH. In the process of enzymolysis, the α-1, 6-glycosidic bonds were hydrolyzed, created hydroxyl groups, and then formed hydrogen bonds. Zhang, Tian, Bai, Xu, and Jin (2013) reported that the bands at 1417 cm^{-1}, 1600 cm^{-1}, and 3400 cm^{-1} also changed during the retrogradation process, suggesting an amorphous region reduction or increase in the structural organization. The intensity at about 960 cm^{-1} was attributed to skeletal mode vibrations of α-1,4 glycosidic linkage (C–O–C), and the peak of the C–O–C

Table 1
Thermal characteristics and crystallinity of proso millet native starch (NS) and nano-scale starch particles prepared with different retrogradation time: 0.5, 4, 12, and 24 h.

Samples	T_o (°C)	T_p (°C)	T_c (°C)	$T_c - T_o$ (°C)	ΔH (J/g)	Crystallinity %
NS	71.87 ± 0.68^{b}	76.74 ± 0.06^{d}	84.07 ± 0.16^{e}	12.20 ± 0.52^{e}	10.29 ± 0.48^{a}	37.22 ± 0.05^{c}
0.5 h	80.36 ± 0.21^{a}	92.12 ± 0.91^{a}	100.32 ± 0.61^{c}	19.96 ± 0.40^{c}	$6.77 \pm 0.35^{b,c}$	42.27 ± 0.84^{b}
4 h	80.24 ± 0.18^{a}	86.93 ± 0.41^{b}	97.25 ± 0.26^{d}	17.01 ± 0.08^{d}	7.18 ± 0.62^{c}	43.02 ± 0.19^{b}
12 h	62.87 ± 0.47^{d}	84.53 ± 0.74^{c}	107.05 ± 0.21^{a}	44.21 ± 0.23^{a}	7.39 ± 0.59^{c}	47.04 ± 0.35^{a}
24 h	65.12 ± 0.04^{c}	78.07 ± 0.64^{d}	103.55 ± 0.56^{b}	38.43 ± 0.52^{b}	8.02 ± 0.47^{b}	46.75 ± 0.30^{a}

All data represent the mean of three determinations.
Mean ± standard deviation.
Means with the same letter in each column are not significantly different ($p < 0.05$).

group of all recrystallized starch nanoparticle samples were more obvious and shifted toward lower wave numbers, from 960 cm^{-1} (NS) to 956 cm^{-1} (0.5 h), 940 cm^{-1} (4 h), 935 cm^{-1} (12 h), and 931 cm^{-1} (24 h), respectively. This indicated that the hydrogen bonds between starch molecular chains in the starch nanoparticles were stronger after reassembling compared to the native starch molecules.

3.4. Differential Scanning Calorimeter (DSC)

The thermal transition behaviors of native proso millet starch and recrystallized starch nanoparticle samples prepared with different retrogradation time are given in Table 1. The gelatinization peak temperatures (T_p) and the conclusion temperatures (T_c) of the nano-scale starch particle samples were higher than those of the native starch. The gelatinization temperature range ($T_c - T_o$) of native starch was 12.20 °C, while the $T_c - T_o$ of the recrystallized starch nanoparticle samples with different retrogradation time was much larger than that of the native starch. The recrystallized sample at 4 °C for 12 h had the highest gelatinization temperature range, at 44.21 °C, while the other samples with 0.5, 4, and 24 h retrogradation time were 19.96 °C, 17.01 °C, and 38.43 °C, respectively. The wider gelatinization temperature range indicated that the recrystallization of debranched starch blocklets and short linear glucans may affect the gelatinization of the crystalline region, suggesting an amorphous region reduction or increase in the structural organization (Zhang, Tian, Bai, Xu, and Jin (2013)). Different reductions were also observed in the endothermic enthalpy (ΔH) of the recrystallized starch nanoparticle samples when compared with the native starch. ΔH reflects the amount of double helical and crystalline order, a parameter that is influenced by amylose content, amylopectin chain-length distribution, and amylose lipid complexes. The ΔH of starch decreased from 10.29 J/g (NS) to 6.77 J/g (0.5 h), 7.18 J/g (4 h), 7.39 J/g (12 h), and 8.02 J/g (24 h), respectively. The decrease in ΔH of the recrystallized starch nanoparticle samples can be explained in terms of decreased ordering and less stabilized double helical structures through hydrogen bonds and other intermolecular forces (Mutungi, Rost, Onyango, Jaros, & Rohm, 2009). Shi et al. (2013) also reported that differences in $T_c - T_o$ may be due to the small recombined crystallites from the cooked-debranched starch with short amylopectin chains; this probably produced several different types of crystallites during storage and saw an increased variation in crystallinity with increasing recrystallization time.

3.5. Thermogravimetric analysis

The TGA curves of native proso millet starch and starch nanoparticle samples recrystallized with different retrogradation time are shown in Fig. 4. TGA and DTG thermograms were used to describe the thermal stability caused by the heating method (Moreira et al., 2013). Three distinct regions can be seen in these thermogravimetric curves. The initial mass loss is generally ascribed to the decomposition of free water in the

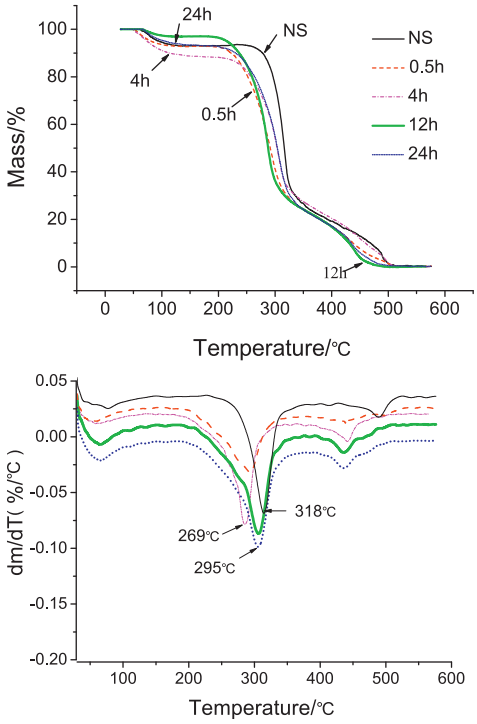

Fig. 4. TGA and DTG thermograms for proso millet native starch (NS) and nano-scale starch particles with different retrogradation time: 0.5, 4, 12, and 24 h.

samples (Tian, Li, Xu, & Jin, 2011). The second stage is the main degradation zone of starch, and the final stage is generally carbonization decomposition. The onset decomposition temperature of the native starch was 318 °C, while the temperatures of the starch nanoparticle samples were much lower and occurred within the range of 269–295 °C. The native starch had a higher onset decomposition temperature than the recrystallized nano-scale starch samples, indicating that the recrystallization of debranched starch enzymatic hydrolysate decreased the stability of the native starch.

As shown in the DTG curve, the nano-scale starch samples decomposed prior to the native starch, indicating lower thermal stability. The decrease in thermal stability could be explained in terms of decreased ordering and the molecular weight of the recrystallized starch nanoparticles during different recrystallization time. Compared with native starch, the bonding interactions among the short amylose were weaker, contributing to the formation of less perfect double helix during the re-association process of the debranched starches. Similarly, biopolymer particles obtained by acid hydrolysis also displayed a decreased thermal stability with an increasing degree of hydrolysis, as evidenced by TGA and DTG (Huang, Yu, & Ma, 2004). Le Corre, Bras, and Dufresne (2010) also reported that the depolymerization of starch nanocrystals made via acid hydrolysis started earlier than that of native starch, which they

attributed to the presence of sulfate groups on the surface of the starch nanocrystals.

4. Conclusions

In this study, starch nanoparticles were prepared from proso millet starch using a green and facile method of pullulanase debranching combined with recrystallization. A series of physical properties of the native starch and starch nanoparticles prepared with different retrogradation time (0.5, 4, 12, and 24 h) were investigated and compared. The results indicated that after debranching with pullulanase and recrystallizing at 4 °C for different storage time, starch nanoparticles with a size between 20 and 100 nm could form. The native starch had an A-type crystal pattern, while the nanoparticle samples showed a B-type crystal pattern and higher relative crystallinity. The characteristics of starch nanoparticles prepared with different retrogradation time were of great difference in many aspects. With the retrogradation time longer, the starch nanoparticles showed higher yield, higher degree of crystallinity and smaller size uniformity. The nanoparticles prepared with a 12 h retrogradation time had the highest degree of crystallinity, at 47.04%, and the highest thermal stability among all nanoparticle samples. What is more, compared to the conventional acid hydrolysis process used to make starch nanoparticles, the present approach has the advantage of being quite rapid and presenting a higher yield (about 55%). Our process offers the advantage of speed and easy implementation, since no chemical reagent is added during the preparing process.

References

An, H. J., Liang, H. B., Liu, Z. D., Yang, H. S., Liu, Q. D., & Wang, H. B. (2011). Nanostructures of debranched potato starch obtained by isoamylolysis. *Journal of Food Science*, *76*(1), 11–14.

Angellier, H., Molina-Boisseau, S., & Dufresne, A. (2005). Mechanical properties of waxy maize starch nanocrystal reinforced natural rubber. *Macromolecules*, *38*(22), 9161–9170.

Buleon, A., Veronese, G., & Putaux, J. L. (2007). Self-association and crystallization of amylose. *Australian Journal of Chemistry*, *60*, 706–718.

Chanvrier, H., Uthayakumaran, S., Appelqvist, I. A. M., Gidley, M. J., Gilbert, E. P., & Lopez-Rubio, A. (2007). Influence of storage conditions on the structure, thermal behaviour and formation of enzyme-resistant starch in extruded starches. *Journal of Agricultural and Food Chemistry*, *55*, 9883–9890.

Geng, J., Jiang, L. P., & Zhu, J. J. (2012). Crystal formation and growth mechanism of inorganic nanomaterials in sonochemical syntheses. *Science China Chemistry*, *55*(11), 2292–2310.

Huang, M. F., Yu, J. G., & Ma, X. F. (2004). Studies on the properties of montmorillonite reinforced thermoplastic starch composites. *Polymer*, *45*, 7017–7023.

Ju, Z. Y., Hettiarachchy, N. S., & Rath, N. (2001). Extraction, denaturation and hydrophobic properties of rice flour proteins. *Journal of Food Science*, *66*, 229–232.

Kim, M. J., Choi, S. J., Shin, S. I., Sohn, M. R., Lee, C. J., & Kim, Y. (2008). Resistant glutarate starch from adlay: Preparation and properties. *Carbohydrate Polymers*, *74*, 787–796.

Kim, S. K., Choi, H. J., Kang, D. K., & Kim, H. Y. (2012). Starch properties of native proso millet (*Panicum miliaceum* L.). *Agronomy Research*, *10*(1–2), 311–318.

Kim, J.-Y., & Lim, S.-T. (2008). Fragmentation of waxy rice starch granules by enzymatic hydrolysis. *Cereal Chemistry*, *85*(2), 182–187.

Kim, J.-Y., & Lim, S.-T. (2009). Preparation of nano-sized starch particles by complex formation with n-butanol. *Carbohydrate Polymers*, *76*, 110–116.

Kunal, P., Banthia, A. K., & Majumdar, D. K. (2008). Effect of heat treatment of starch on the properties of the starch hydrogels. *Materials Letters*, *62*, 215–218.

Le Corre, D., Bras, J., & Dufresne, A. (2010). Starch nanoparticles: A review. *Biomacromolecules*, *11*, 1139–1153.

Lian, X. J., Liu, L. Z., Guo, J. J., Li, L., & Wu, C. Y. (2013). Screening of seeds prepared from retrograded potato starch to increase retrogradation rate of maize starch. *International Journal of Biological Macromolecules*, *60*, 181–185.

Lin, J.-H., & Chang, Y.-H. (2006). Effects of type and concentration of polyols on the molecular structure of corn starch kneaded with pullulanase in a Farinograph. *Food Hydrocolloids*, *20*, 340–347.

Liu, D. G., Wu, Q. L., Chen, H. H., & Chang, P. R. (2009). Transitional properties of starch colloid with particle size reduction from micro- to nanometer. *Journal of Colloid and Interface Science*, *339*, 117–124.

Milasinovic, M. S., Radosavljevic, M. M., & Dokic, L. P. (2010). Effects of autoclaving and pullulanase debranching on the resistant starch yield of normal maize starch. *Journal of the Serbian Chemical Society*, *75*(4), 449–458.

Miao, M., Jiang, B., & Zhang, T. (2009). Effect of pullulanase debranching and recrystallization on structure and digestibility of waxy maize starch. *Carbohydrate Polymers*, *76*, 214–221.

Moreira, F. K., Pedro, D. C., Glenn, G. M., Marconcini, J. M., & Mattoso, L. H. (2013). Brucite nanoplates reinforced starch bionanocomposites. *Carbohydrate Polymers*, *92*, 1743–1751.

Mutungi, C., Rost, F., Onyango, C., Jaros, D., & Rohm, H. (2009). Crystallinity, thermal and morphological characteristics of resistant starch type III produced by hydrothermal treatment of debranched cassava starch. *Starch/Stärke*, *61*(11), 634–645.

Putaux, J. L., Molina-Boisseau, S., Momaur, T., & Dufresne, A. (2003). Platelet nanocrystals resulting from the disruption of waxy maize starch granules by acid hydrolysis. *Biomacromolecules*, *4*(5), 1198–1202.

Santhanee, P.-A., & Dudsadee, U. (2013). Rice starch vs. rice flour: Differences in their properties when modified by heat-moisture treatment. *Carbohydrate Polymers*, *91*, 85–91.

Shamai, K., Bianco-Peled, H., & Shimoni, E. (2003). Polymorphism of resistant starch type III. *Carbohydrate Polymers*, *54*, 363–369.

Shi, M. M., Chen, Y., Yu, S. J., & Gao, Q. Y. (2013). Preparation and properties of RS III from waxy maize starch with pullulanase. *Food Hydrocolloids*, *33*, 19–25.

Shi, M. M., & Gao, Q. Y. (2011). Physicochemical properties, structure and in vitro digestion of resistant starch from waxy rice starch. *Carbohydrate Polymers*, *84*, 1151–1157.

Shi, A.-M., Wang, L.-J., Li, D., & Benu, A. (2012). The effect of annealing and cryoprotectants on the properties of vacuum-freeze dried starch nanoparticles. *Carbohydrate Polymers*, *88*, 1334–1341.

Simsek, S., & El, S. N. (2012). Production of resistant starch from taro (*Colocasia esculenta* L Schott) corm and determination of its effects on health by in vitro methods. *Carbohydrate Polymers*, *90*, 1204–1209.

Tari, T. A., Annapure, U. S., Singhal, R. S., & Kulkarni, P. R. (2003). Starch-based spherical aggregates: Screening of small granule sized starches for entrapment of a model flavouring compound, vanillin. *Carbohydrate Polymers*, *53*(1), 45–51.

Tian, Y. Q., Li, Y., Xu, X. M., & Jin, Z. Y. (2011). Starch retrogradation studied by thermogravimetric analysis (TGA). *Carbohydrate Polymers*, *84*, 1165–1168.

Watcharatewinkul, Y., Puttanlek, C., Rungsardthong, V., & Uttapap, D. (2009). Pasting properties of a heat-moisture treated canna starch in relation to its structural characteristics. *Carbohydrate Polymers*, *75*, 505–511.

Yañez, G. A., Walker, C. E., & Nelson, L. A. (1991). Some chemical and physical properties of proso millet (Panicum milliaceum) starch. *Journal of Cereal Science*, *13*(3), 299–305.

Young-Il Cho, Chung Jong-Wook, Lee Gi-An, Ma Kyung-Ho, Dixit Anupam, Gwag Jae-Gyun, & Park Yong-Jin. (2010). Development and characterization of twenty-five new polymorphic microsatellite markers in proso millet (*Panicum miliaceum* L.). *Genes & Genomics*, *32*, 267–273.

Zhang, H., & Jin, Z. (2011). Preparation of products rich in resistant starch from maize starch by an enzymatic method. *Carbohydrate Polymers*, *86*, 1610–1614.

Zhang, H. X., Tian, Y. Q., Bai, Y. X., Xu, X. M., & Jin, Z. Y. (2013). Structure and properties of maize starch processed with a combination of α-amylase and pullulanase. *International Journal of Biological Macromolecules*, *52*, 38–44.